

RESEARCH ARTICLE

## **Allamanda cathartica L. Latex Mediated Magnesium Oxide Nanoparticles as Antiproliferative Agents.**

**Kiranmayee Pamidimukkala\*, Prabhudas Nelaturi, Nandini Huthur Sriramaiah and Kutty Ambalath Veetilveeran Moideen**

Department of Cell Biology and Molecular Genetics, Sri Devaraj Urs Academy of Higher Education and Research, Tamaka- 563 103, Kolar, Karnataka, India.

### ARTICLE INFO

#### Article History:

Received 11 May 2021

Accepted 23 Jul 2021

Published 01 Aug 2021

#### Keywords:

Genotoxicity

nanomagnesium

trypan blue

phytochemicals

human peripheral

blood mononuclear cells.

### ABSTRACT

Green based nanoparticles were synthesized to investigate the cytotoxic effects on human peripheral blood mononuclear cells (hPBMCs). Nanoparticles were made by mixing aqueous *Allamanda cathartica* L. latex (3%) and magnesium oxide (1mM) at 37°C on shaker for 24 hours. The developed nanoparticles were characterized by Scanning Electron Microscopy, Transmission Electron Microscopy, Fourier Transmission Infra-Red, Zeta potential and X-ray diffraction. hPBMCs were tested *in vitro* with different concentrations of synthesized nanoparticles and found that 100 µg/mL showed about 96% dead cells from trypan blue dye exclusion method. Though controlling the proliferation of cells, the nanoparticles did not exhibit any genotoxicity, indicating that the nanoparticles showed their effect on the periphery of the cells, breaking them and leading to cell death. This is the first report of green route development of MgO nanoparticles using the latex of *Allamanda cathartica* L. and finding their efficacy on hPBMCs. Further analysis is required to confirm their use as therapeutics in leukemia.

### How to cite this article

Pamidimukkala K., Nelaturi P., Huthur Sriramaiah N., Ambalath Veetilveeran Moideen K. *Allamanda cathartica* L. Latex Mediated Magnesium Oxide Nanoparticles as Antiproliferative Agents.. *Nanomed Res J*, 2021; 6(3): 257-268. DOI: 10.22034/nmrj.2021.03.006

### INTRODUCTION

During the twenty-first century, nanoparticles (NPs) in nanotechnology have gained importance in multidisciplinary fields; broadly, medicine, agriculture, energy science, engineering and so on. The growing interest in preparation of these nanoparticles is mainly valued the environment and other living beings. Use of metals in nanoparticle synthesis is an advantage since these metals are somewhere or the other linked to the body's functions. The various metabolic activities of a living system are controlled by enzymes; their functions are regulated by the cofactors, such as zinc, copper, iron, potassium, calcium and magnesium. Inorganic based metal and metal oxide nanoparticles are in practice with silver, titanium, zinc, copper etc [1] (Jeevanandam et al.

2018). In recent past, the antioxidant properties of NPs, for example, nanomagnesium, nanosilver, nanozinc, nanoselenium and so on have been proved to have oxidation reducing capacity in diabetes, cardiotoxicity, diabetes neuropathy and so on [2] (Heydary et al. 2015). Metal oxides, in spite of having many modes of nanoparticle synthesis, are widely accepted in "green synthesis", which means, synthesizing nanoparticles with biological sources from microscopic algae to macroscopic plants. Green approach is not only easy but also rapid, cost effective and eco friendly. Several types of plant derived chemicals, called phytochemicals, include proteins, alkaloids, phenolic compounds, tannins, glycosides and polysaccharides participate in nanoparticle synthesis, thus considered as safe. These compounds involve the bio-reduction of metals and their oxides at the time of eco-friendly

\* Corresponding Author Email: [kiranmayee@sduu.ac.in](mailto:kiranmayee@sduu.ac.in)

nanoparticle formation. Green nanotechnology uses and develops nano sized particles by blending metals with plant material. The synthesized particle size is smaller than 100 nanometers. Many previous studies authenticated from the research that the synthesized nanoparticles limit oxidative stress, genotoxicity and apoptotic activities [3] (Kuppusamy et al. 2016). Magnesium oxide (MgO) is widely used metal oxide in non-medical fields (cosmetics, electrical insulation, food packaging industry, desiccation units) [2] (Heydary et al. 2015). It is a thermostable, inexpensive and biologically compatible metal. In healthcare, MgO has antibacterial properties. It is a part of antacid (relieves heartburn), laxative (short term), quick emptying of the bowel (just before surgery), also used as dietary supplement and MgO is recognized as safe/ non-toxic by the U.S. Food and Drug Administration (21CFR184.1431) [4] (Cai et al. 2018). Keeping in mind the uses of MgO in healthcare, an attempt has been made for preparing MgO nanoparticles (MgONPs) by using latex from *Allamanda cathartica* L., a medicinal plant. In the plant kingdom, only a limited number of plants produce latex and one among them is *A. cathartica* L., belonging to the family Apocynaceae. Latex is a rich source of glycosides, saponins, alkaloids, tannins and other phytochemicals [5] (Kiranmayee et al. 2020). In addition to other essential phytochemicals, the whole plant of *A. cathartica* contains plumieride, plumericin, and allamandin. The isolated and identified chemical constituents from leaves are ursolic acid,  $\beta$ -sitosterol,  $\beta$ -amyrin, plumericin, sesquiterpenes, and plumieride. Along with the above, stem and bark contain triterpenoids, glucoside, and alkaloids. Whereas flowers contain kaempferol, quercetin and other flavonoid compounds; roots are rich with triterpenoids, plumieride, alkaloid and glucoside. The whole plant shows ethanopharmacological properties. To name a few, laxative, an antibiotic, treats malaria, jaundice, enlarged spleen, cough, anti-inflammatory, purgative, antioxidant properties. Sap contains antibacterial and anticancer properties [6] (Chandreyi et al. 2019). Hyperglycemia and Mg deficit are common in type 2 diabetes. Glucose and insulin are the key regulators in Mg metabolism [7] (Mario and Ligia 2015). Because of its poor bioavailability, MgO gets putrefied by digestive juices and acids. The best way to escape from this and increase bioavailability is to use MgO nanoparticles, in

particular, synthesized by green approach [8] (Patil 2020). As human Peripheral Blood Mononuclear Cells (hPBMCs) are having direct contact with NPs, in the present study MgONPs were made by adopting a green approach. Normal cell and tissue protein denaturation is the side effect of NPs. Based on the medicinal properties of plant latex and the metal, MgO nanoparticles were synthesized by green approach. The synthesized particles were characterized by the standard methods, and tested their genotoxic efficacy on hPBMCs. As far as our knowledge is concerned, this is the first report of using *A. cathartica* latex and MgO for green route development of nanoparticles and finding their efficacy on hPBMCs.

## MATERIALS AND METHODS

The plant, *A. cathartica* (golden trumpet), growing on Sri Devaraj Urs Academy of Higher Education and Research, Kolar campus has been identified by Dr. Kiranmayee (one of the authors of this paper) and authenticated again by Horticulture college, Kolar. Specimen was submitted to Dr. Madhava Chetty, Department of Botany, Sri Venkateswara University, Tirupati and obtained voucher specimen number as 0109. The trimmed young twigs were gathered at morning hours to collect latex and stored at 4°C till NP synthesis. By following Harbourne's protocol, phytochemical analyses for alkaloids, flavonoids, saponins, tannins, glycosides, reducing sugars were carried out from 3% latex [9] (Harborne 1973).

### Nanoparticle synthesis

Equal proportions of MgO (1mM) and latex (3%) were mixed till latex is completely solubilized in MgO solution and facilitated the conditions (37°C, 135 rpm, 24 h) for nanoparticle development [10] (Banerjee et al. 2014). The suspension was clarified at 10,000 rpm for 10 min and the pellet was stored at 4°C till further use.

### Characterization of latex nanoparticles

All the characterization studies were carried out in the department of Microbiology and Cell Biology (MCBL) and Spectroscopy Analytical Test Facility and Materials Research Center (MRC), Indian Institute of Science (IISc), Bangalore, Karnataka, India. From the UV-Visible spectrophotometer (Nanodrop 8000), absorption/particle spectrum was obtained between 200 and 700 nm. For Scanning Electron Microscopy (SEM)

and Transmission Electron Microscopy (TEM) [11] (de F Navarro Schmidt 2006), the particles were centrifuged at 4000 rpm for 20 min. Carefully transferred the dried pellet onto a clean slide and images were captured in a SEM, Quanta (200 FEI). For TEM, metal coated copper grids were filled, dried with 10  $\mu$ L NPs and images were captured by tecnai G2 Sprit Bio TWIN at a voltage of 120 kV [12] (Strober 2001). The following were applied to get X-ray diffraction (XRD) data: Bragg angle  $2\theta$  at 2/min scan rate, Seifert Rayflex 300TT X-ray diffractometer, CuK ( $\lambda = 1.542 \text{ \AA}$ ) radiation, 40kV voltage, 30mA current. Zeta potential/ scattered light intensity and particle size distribution were carried out on Horiba Scientific SZ-100. This helped us to measure and confirm the nanoparticle size distribution. Nicolet 6700 Fourier Transform Infrared Radiation (FRIT) was used to get the functional group information by using potassium bromide pellets at a range of  $400^{-1}\text{cm}$  to  $4000 \text{ cm}^{-1}$ .

#### *hPBMC collection and trypan blue dye exclusion*

Since PBMCs are being isolated from human blood, we obtained ethics clearance (SDUAHER/KRL/Res. Project/128/ 2017-'18) from the institute ethics clearance department. The volunteer's blood was collected to isolate hPBMCs by Ficoll gradient method as per the protocol without any alteration [12] (Strober 2001). After the treatment (Table 1), equal volumes of the cells and 0.4% trypan blue were mixed and left at room temperature ( $37^{\circ}\text{C}$ ) for 10 min and 10  $\mu$ L of undisturbed suspension was used to count the viable and non-viable cells in the hemocytometer.

Viability % =  $\frac{\text{Number of cells}}{\text{Total number of cells}} \times 100$

#### *Effect of nanoparticles on DNA*

By hemocytometer, cells were counted ( $10^4$ ) and subjected to DNA fragmentation assay [13] (Pattern and Hirzel 2017). Pelleted cells were lysed

in 20  $\mu$ L of TES buffer (Tris-1M, EDTA-20mM and SDS-1%), added 10  $\mu$ L each of RNase and proteinase K, incubated at  $37^{\circ}\text{C}$  for 1 h and  $50^{\circ}\text{C}$  for 1 hour and 30 min respectively. Spun down the sample, the entire supernatant was mixed with 6 X DNA loading dye, ran the agarose gel at 80 volts and documented the image.

#### *Statistical analysis*

Performed the experiments for three times, their averages were presented to minimize the errors.

## RESULTS AND DISCUSSION

Without any complexity, the present study focused on NP synthesis by using easily available *A. cathartica* latex and MgO. When mixed and incubated equal proportions of 1 mM MgO and 3% aqueous latex, initial colourless solution turned into bottle green colour (Fig. 1), indicating that the phytochemicals of latex have been reduced and became solubilizing agents for the formation of MgO nanoparticles.

#### *Characterization of particles was carried out by UV-Visible spectrophotometry, FTIR, SEM, TEM and Zeta potential*

Metal nanoparticles are good conductors and have plasmon resonance. The size of metal nanoparticles and light absorption are directly proportional to each other [14] (Kelly et al. 2003). This is the most widely used method to find the absorption spectra of nanoparticles, because the bands/peaks are correlated to diameter and the ratio of metal nanoparticles [15] (Philip 2008). Before the efficacy check, the green MgONPs were characterized by spectrophotometry. This gives the peak concentration. The nanoparticle size between 2 and 100 nm is conveniently measured at wavelengths between 300 and 800 [16] (David and Vanden Bout 2002). The absorption peak at

Table 1. Details of controls and treatments used in the present study

Controls	Treatments
Only PBMCs	MgONPs (20 $\mu\text{g}/\text{mL}$ )
PBMCs + DMSO (20 $\mu\text{L}$ )	MgONPs (40 $\mu\text{g}/\text{mL}$ )
PBMCs + DMSO (100 $\mu\text{L}$ )	MgONPs (60 $\mu\text{g}/\text{mL}$ )
PBMCs + 1mM metal solution (20 $\mu\text{L}$ )	MgONPs (80 $\mu\text{g}/\text{mL}$ )
PBMCs + 1mM metal solution (100 $\mu\text{L}$ )	MgONPs (100 $\mu\text{g}/\text{mL}$ )
PBMCs + 3% latex (20 $\mu\text{L}$ )	
PBMCs + 3% latex (100 $\mu\text{L}$ )	



Fig. 1. Development of nanoparticles when mixed equal proportions of 1mM MgO and 3% latex.  
 A. Collection of latex from young twig, B. Collected latex on ice, C. Developed nanoparticles

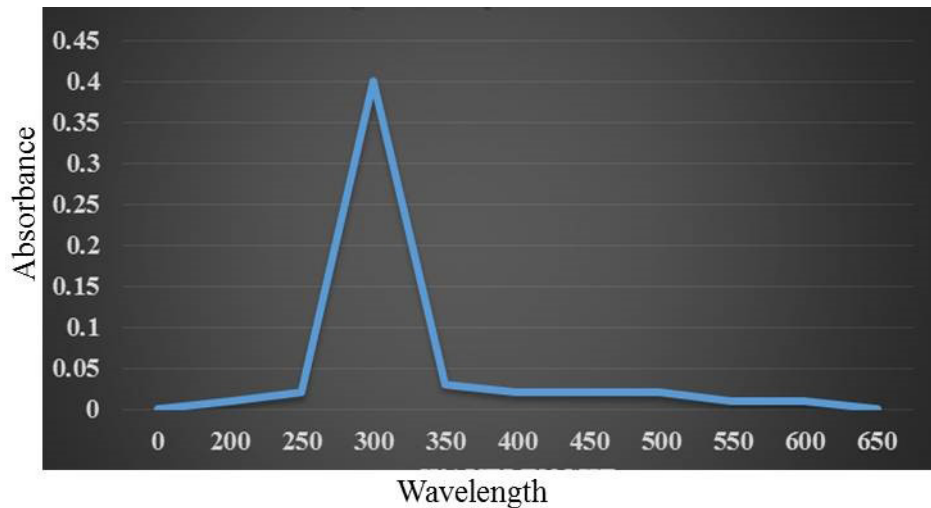


Fig. 2. UV-Visible spectrum of MgONPs with maximum absorption peak at 329nm indicates the development of MgONPs.

329 nm is the characterization of plasma resonance of synthesized MgONPs (Fig. 2), proven the development of nanoparticles UV-V is peak at 329 nm clarifies the reduction of latex phytochemicals and able to form MgONPs. As shown (Fig. 2), the absorption maximum was noted roughly at 329 nm, which coincided with another study [17] (Renata Dobrucka 2018). Further confirmation was carried out by SEM, TEM, FTIR and X-RD analyses.

FTIR spectroscopy helps to identify the likely biomolecules/phytochemicals responsible for the reduction and capping of the MgONPs. Also, helps to know the possible interaction between metal and the phytochemicals. The spectrum (Fig. 3) was taken between 4000 and 400  $\text{cm}^{-1}$ . The broad

and strong peak at 3149  $\text{cm}^{-1}$  is a stretching of the O-H group in an alcohol, which is a carboxylic acid [17] (Renata Dobrucka 2018) and a small peak at 2352.23 is due to O=C=O stretch. The results are synchronized with Ahmed et al. [18] (Halbus Ahmed *et al.* 2019).

SEM scans the surface and produces images of any sample that scans. The morphology of MgONPs obtained from SEM is shown in Fig. 4. The scale bar was 10  $\mu\text{m}$ , 20, 50, 100 and 300  $\mu\text{m}$ . The particles were in mass like and formed large clusters as mentioned in the previous study [17] (Renata Dobrucka 2018).

In TEM, a beam of electron scans the sample, detects the sample's surface topology and provides

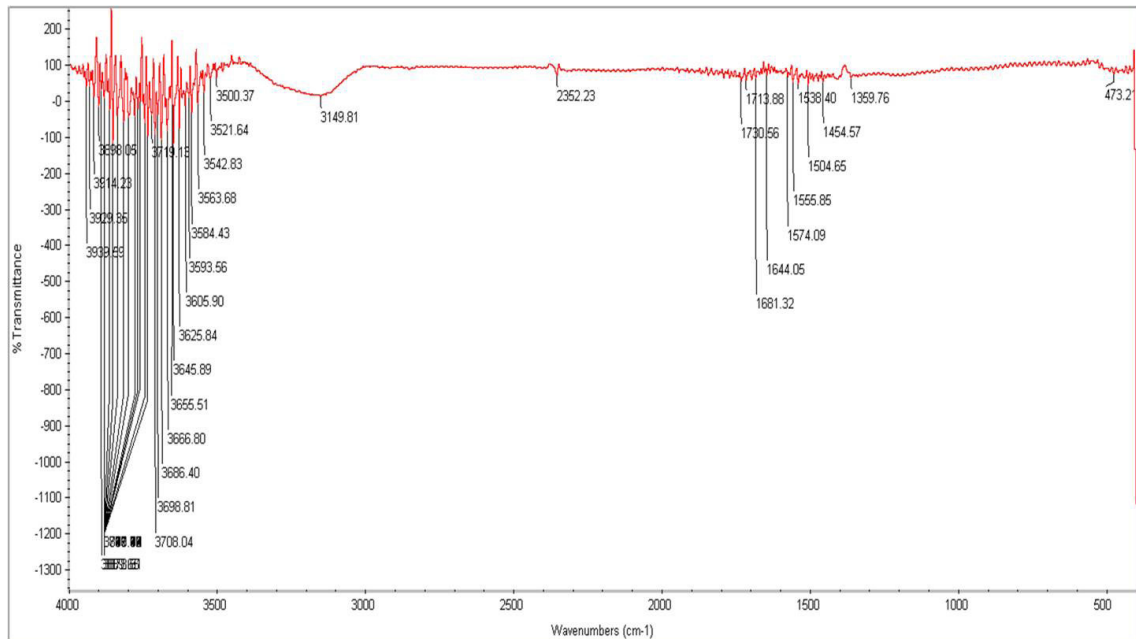


Fig. 3. Showing FTIR spectrum of synthesized MgONPs with bonds corresponding to the capping phytochemicals from the latex.

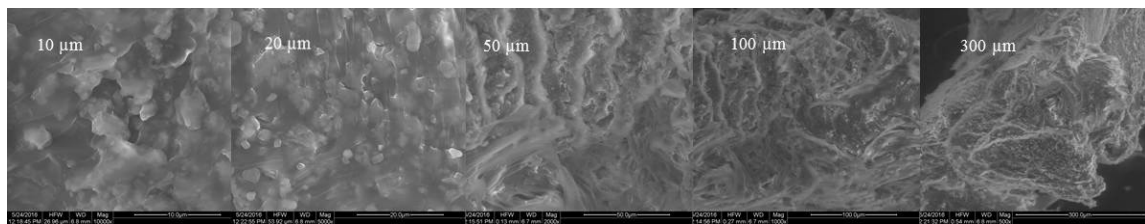


Fig. 4. Scanning Electron Microscopic images of the MgONPs. The numbers indicate the scale at which the particles were captured.

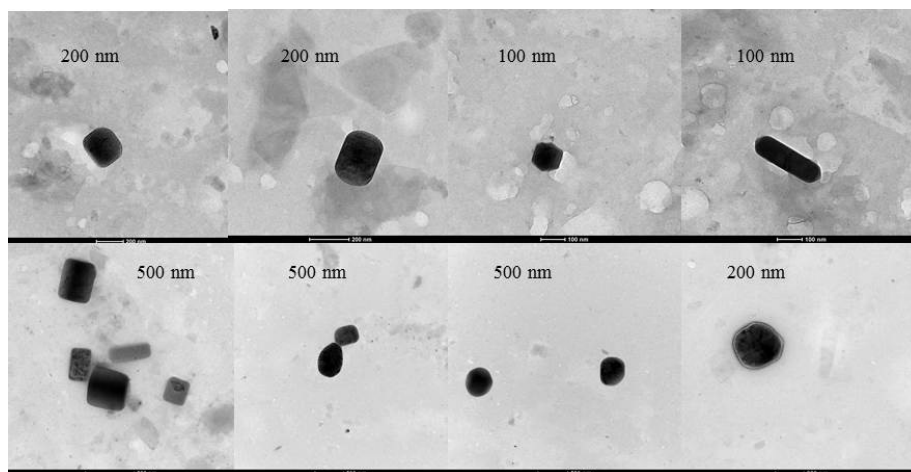


Fig. 5. Transmission Electron Microscopic images of the MgONPs. The numbers indicate the scale of the captured NPs.

the shape and size. In the present study, the shapes of MgONPs noted were spherical, cylindrical, rectangular, hexagonal and round; the measured area, angle, length and diameter of the particles

were shown (Fig. 5). About 36 particles were measured and the average particle size was noted as 32.3 nm. The minimum and maximum sizes noted were 10.6 and 61.3 respectively (Table 2).

Zeta potential/ scattered light intensity and particle size distribution were carried out on Horiba Scientific SZ-100. This helped us to measure and confirm the nanoparticle size distribution (Fig. 6).

MgONPs XRD analysis was carried out and

XRD analysis of the synthesized particles helped us to understand the crystal nature. (X-ray tube: Empyrean Cu LFF (9430 033 7300x) DK400339, Filter: Beta-filter Nickel, Detector: PIXcel-1D detector) (Fig. 7).

*Cytotoxicity on hPBMCs*

Table 2. MgONPs were measured from Image J software. About 36 particles were measured and the average particle size was noted as 32.3 nm. The minimum and maximum sizes noted were 10.6 and 61.3 respectively.

Area	Mean	Min	Max	Angle	Length	Diameter
1.19	76.402	45.864	162	101.689	11.846	
88	75.749	38	219	0	0	10.6
1.31	66.926	32.87	204.651	100.62	13.023	
112.88	74.226	8	224	0	0	12
2.13	31.544	0	198	54.211	21.204	17.3
234.32	48.455	0	228	0	0	
2.53	26.343	3.531	100	0	0	19.4
2.55	45.262	19.711	163.205	123.44	25.406	
316.97	51.541	11	109	0	0	20.1
2.27	60.725	30.344	227.934	52.927	22.56	
325.14	66.444	14	249	0	0	20.3
22.2	10.652	0	169	49.399	22.12	
337.84	17.503	0	203	0	0	20.7
2.16	54.281	29.291	221	46.507	21.503	
359.92	71.762	14	249	0	0	21.4
2.55	23.173	4.008	90.984	102.724	25.424	
371.18	28.644	0	188	0	0	21.7
2.63	87.095	49.052	153	111.477	26.221	
413.83	96.082	21	249	0	0	23
2.6	18.294	0	197	58.276	25.864	
483.72	43.388	0	233	0	0	24.8
2.77	38.699	0	237.129	76.569	27.554	
488.48	46.86	0	253	0	0	24.9
3.13	16.948	0	194	87.064	31.241	
514.33	22.339	0	240	0	0	25.6
3.09	14.744	0	190	89.256	30.803	
528.26	21.033	0	222	0	0	25.9
2.94	64.638	20.14	148.214	85.301	29.298	
535.2	77.351	9	230	0	0	26.1
3.71	103.838	84.368	180	9.972	36.958	
533.65	115.046	71	209	0	0	26.1
287	43.527	2.501	133	11.31	28.555	
583.35	61.857	0	245	0	0	27.3
3.02	39.055	0	207	76.149	30.075	
598.2	45.305	0	254	0	0	27.6
3.65	40.724	0	185.341	92.517	36.435	
932.49	54.39	0	254	0	0	34.5
3.84	40.09	0	114	111.468	38.254	
934.48	41.535	0	211	0	0	34.5
3.69	38.866	0	169.587	78.079	36.793	
972.08	42.037	0	244	0	0	35.2
4.13	41.826	1.141	156	55.692	41.161	
982.91	49.146	0	254	0	0	35.4
4.13	16.096	0	131.173	97.815	41.183	
1122.47	34.805	0	195	0	0	37.8
5.44	12.406	0	205.604	74.634	54.343	
1126.36	14.848	0	186	0	0	37.9
4.47	38.008	0.69	198.243	112.659	44.646	
1127.08	50.974	0	254	0	0	37.9
4.4	50.579	5.635	133.722	145.008	43.944	
1217.77	58.975	0	254	0	0	39.4
6.43	26.146	0.333	121.232	145.914	64.236	

Continued Table 2. MgONPs were measured from Image J software. About 36 particles were measured and the average particle size was noted as 32.3 nm. The minimum and maximum sizes noted were 10.6 and 61.3 respectively.

Area	Mean	Min	Max	Angle	Length	Diameter
1223.39	39.38	0	254	0	0	39.5
4.58	36.618	0	114.919	118.811	45.651	
1230.48	41.043	0	224	0	0	39.6
4.71	31.842	0	229.858	80.698	47.018	
1381.44	55.367	0	254	0	0	41
4.33	41.523	1.343	177.778	92.651	43.246	
1410.76	50.624	0	212	0	0	42.4
4.17	40.033	0	169.728	103.903	41.619	
1475.47	52.599	0	246	0	0	43.3
5.02	35.336	0	225.069	100.592	50.053	
1666.66	47.819	0	254	0	0	46.1
5.11	41.667	0	174	114.555	51.041	
1804.96	64.973	0	254	0	0	47.9
6.89	34.656	0	185.101	70.301	68.828	
2561.82	52.675	0	216	0	0	57.1
6.59	39.239	0	190.193	27.499	65.839	
2575.58	55.071	0	235	0	0	57.3
6.27	42.367	0.913	159.301	110.171	62.642	
2948.35	61.159	0	254	0	0	61.3

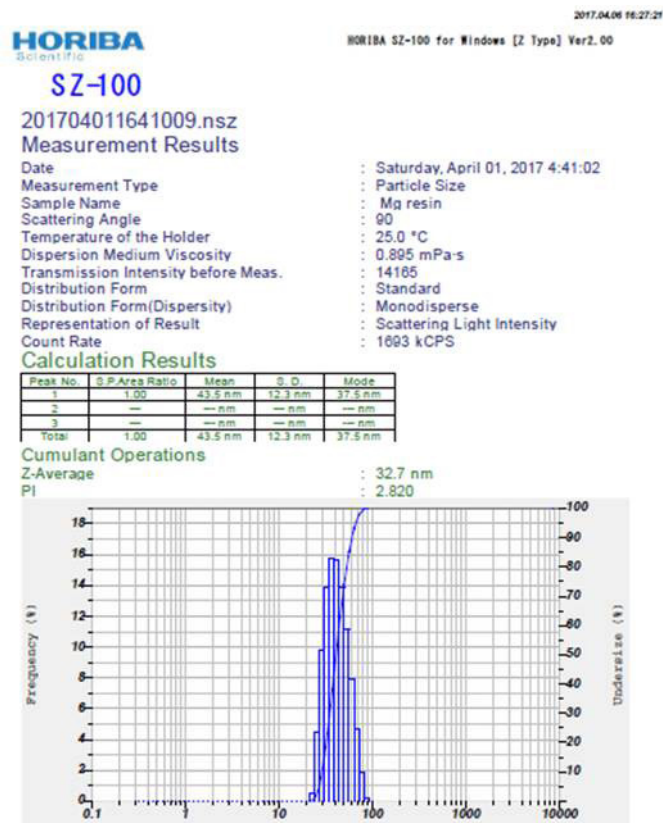


Fig. 6. Particle size analysis histogram with intensity distribution of MgONPs for particles size

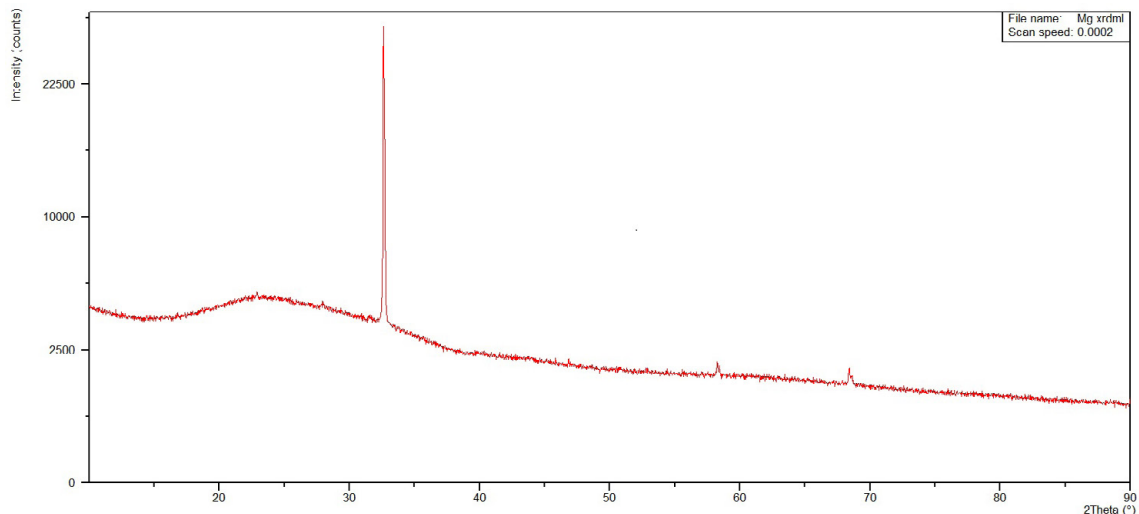


Fig. 7. X-ray diffraction analysis of MgONPs

The effect of MgONPs on hPBMCs was tested at 20  $\mu\text{g/mL}$ , 40, 60, 80, and 100  $\mu\text{g/mL}$  concentrations. At 72 h, cell viability percentage was assessed with trypan blue dye exclusion method. Increased concentration showed decreased viable cell percentage. The comparative data among the treatments was shown (Table 3).

In recent years, nanoparticle based drug delivery systems have attained much attention. These high efficient nanoparticles are being synthesized or fabricated under suitable and ordinary conditions. Because of having large surface area, the synthesized particles have efficient biological interactions in the *in vitro* model. Many research findings open up new avenues as NPs can be customized to induce antiproliferative action against cancer cells. They mediate the formation of reactive oxygen species and induce apoptosis and necrosis [19] (Vinardell and Mitjans 2015). NPs have high accessible area to relate to cell and other organelle membranes. Due to this property, membrane leakage happens and cancer cells induce ablation. Therefore, researchers focus on nanoparticle mediated therapeutics in cancers, most often, the NPs-derived anticancer drugs [20] (Behzadi et al. 2018). In the present study an exploration of the latex mediated MgONPs *in vitro* model by using hPBMCs was done. This will give an overview of understanding the fate of NPs in an *in vivo* model, when used to control proliferative activity of lymphocytes in leukemia. The potential activity of MgONPs as antimicrobial agents and their usage in drug delivery have been elucidated in many reports, but not been explored on hPBMCs.

Many studies reported the possibility of preparing MgONPs from plant and its derivatives. These have proven their antimicrobial activity and wide range of effects on humans. The safe and unsafe use of NPs depends on the size, surface area, conditions used for their formation, concentration etc [21] (Mohsen Safaei et al. 2019). With respect to this, we used different concentrations of MgONPs on hPBMCs and noted the viable and non-viable cells.

The main apprehension about any drug is its distinguishing nature between normal and cancer cells. To keep this in mind, many researchers use green nanoparticles with maximum surface area and having potential antiproliferative effects [21] (Mohsen Safaei et al. 2019). When the particles are internalized into any cell, they act either on cytosol or on nucleus. If they are capable of entering into the nucleus, they may show DNA damage. If this occurs, then the DNA becomes a ladder pattern and subsequently the cell will collapse. To show the resultant action of MgONPs on DNA, we lysed the cells in lysis buffer and loaded in 1% agarose gel (Fig. 8). Unlike other metals [5] (Kiranmayee et al. 2020), the DNA fragmentation pattern indicates that there was neither shearing nor breaking of DNA into fragments. This might indicate that the increased concentration of MgONPs showed decreased percentage of viable cells, signified that the particles did not show any effect on DNA and instead, killed the cells just by bursting them. According to a report by Stoimenov et al., MgONPs exhibited antibacterial activity by bursting the membrane [22] (Peter Stoimenov

Table 3. Per cent live and dead cells of hPBMCs when treated with latex MgONPs.

Treatment	Per cent	
	Live	Dead
Control (only PBMCs)	81.5	18.5
DMSO (20 $\mu$ L)	77	23
DMSO (100 $\mu$ L)	62.5	37.3
Latex (3%) (20 $\mu$ L)	67.6	32.4
Latex (3%) (100 $\mu$ L)	71.7	28.3
Metal (1mM) (20 $\mu$ L)	66.7	33.3
Metal (1mM) (100 $\mu$ L)	52.6	47.3
Treatment 1 (20 $\mu$ g)	65.6	34.4
Treatment 1 (40 $\mu$ g)	53.1	47
Treatment 1 (60 $\mu$ g)	33.3	66.7
Treatment 1 (80 $\mu$ g)	21.7	78.3
Treatment 1 (100 $\mu$ g)	38.5	96

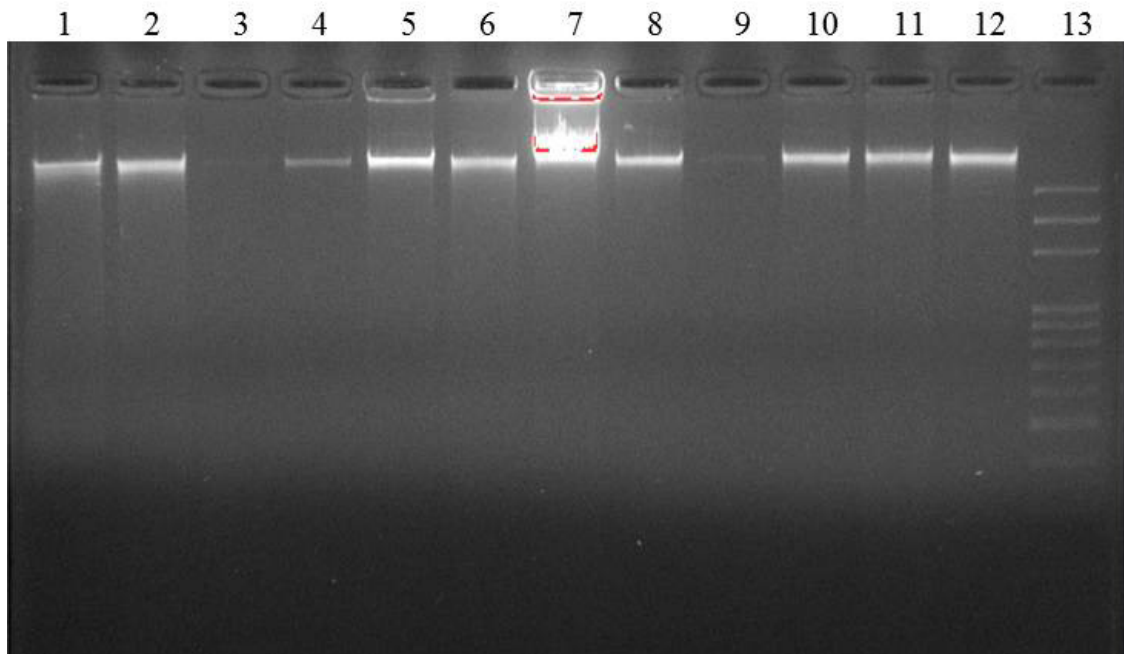


Fig. 8. Agarose gel showing DNA fragmentation pattern of hPBMCs treated with MgONPs. NPs were prepared by mixing 3% latex and 1 mM metals.

From left to right lanes in all the Figs. 1. Control (only PBMCs), lane 2. DMSO (20  $\mu$ L), lane 3. DMSO (100  $\mu$ L), lane 4. Latex (20  $\mu$ L), lane 5. Latex (100  $\mu$ L), lane 6. metal solution (20  $\mu$ L), lane 7. metal solution (100  $\mu$ L), lane 8. 20  $\mu$ g/mL MgONPs, lane 9. 40  $\mu$ g/mL MgONPs, lane 10. 60  $\mu$ g/mL MgONPs, lane 11. 80  $\mu$ g/mL MgONPs, lane 12. 100  $\mu$ g/mL MgONPs, and lane 13. DNA ladder.

et al. 2002). Present results are in coordination with Stoimenov, where MgONPs made from latex affected the cell membrane. In other experimental conditions [23, 24] (Ge et al. 2011; Karthikenyam Krishnamoorthy et al. 2012), cytotoxicity of MgONPs was observed in cancer cells at 200  $\mu$ g/mL and 300  $\mu$ g/mL, however, in our experiment,

the maximum concentration used was 100  $\mu$ g/mL with per cent non-viable cells of 96. Though MgONPs have many applications, limited literature is available on its effect on hPBMCs. Reports are available on cytotoxicity of human umbilical vein endothelial cells [20] (Behzadi et al. 2018), human cardiac microvascular

endothelial cells [25] (Sun et al. 2011), less toxic effects against human astrocytoma U87 cells [26] (Lai et al. 2008), applied MgO nano-shells in cancer therapy [27] (Martinez Boubeta et al. 2010). MgONPs have been used as hyperthermia agents and biosensor in liver cancer treatment [28, 29] (Chalkidou et al. 2011; Lei et al. 2012). Machine dependent study on the harmfulness of MgO nanoparticles to cancer cells and MgONPs were recently been applied in nano-cryosurgery in tumor management [30] (Di et al. 2012). All these investigations support the fact that MgONPs show cytotoxic effects on cancer cells not limited to hPBMCs. Based on the preceding *in vitro* and *in vivo* studies, NPs show a wide variety of sound effects on humans. For functional execution, the NPs shall have nano range size, larger surface area, period of exposure for NPs synthesis, functional group adherence from the plant source and stability. All these properties specify whether the synthesized NPs have safety feature or not. In review, a few published articles proved their toxic nature and a few showed their positive effects and all these are under the survivalance of concentration and the size of MgONPs. Therefore, in the present study, we tested different concentrations of MgONPs on hPBMCs. Contrary to Ge [23] (Ge et al. 2011), we reported lower concentration (100 µg/mL) promoted the death of cells. Using low concentration was advantageous and coinciding with other studies [26, 31], (Lai 2008 et al.; Hasbullah et al. 2013). Taken together the literature survey and the present study results, green approached MgONPs's usefulness and harmfulness on hPBMCs depend on phytochemicals of latex, composition of these phytochemicals, particle concentration, size and the target cells [2] (Heydary et al. 2015). Documentations claim that NPs have high adsorption potential to plasma proteins. Since MgONPs are the potential drug delivery candidates, having magnetic resonance image and suitable even at failed thermoregulation situations, exploration is needed to test against human chronic myelogenous leukemia and safety assessment of human serum albumin (HSA) as it contributes the formation of protein corona on the NPs [32] (Lesniak et al. 2012). To conclude from the present research results from latex mediated MgONPs on hPBMCs, these particles have a potential role in antiproliferative activity.

## CONCLUSION AND LIMITATION

*Allamanda cathartica* latex, which can be collected from the trimmed twigs and MgO, which is available at low cost, are good sources of synthesizing nanoparticles on shaker at 37°C. The authors used 3% aqueous latex and 1 mM MgO for NP synthesis. The colourless solution turned to bottle green colour indicated the plant latex has been reduced and became a stabilizing agent for MgONPs. The biophysical characterization techniques proved the biosynthesis of MgONPs. On an average, the particle size noted was 32 nm, which is a suitable particle to target the cells to be examined. When using latex MgONPs, an increased percentage of non-viable hPBMC cells were noted at as low as 100 µg/mL. Though nanoparticles did not fragment DNA, particles might stick to the cells, burst open the cells and finally led to cell death. Therefore, low concentration of latex mediated MgONPs can play antiproliferative role on cells. White blood cell number will be high in leukemic condition. Much research is needed to prove that latex mediated MgONPs might be a good source to control leukemic cells. Limitation of the study was to check the effectiveness of these green MgONPs on Leukemia cells.

## ACKNOWLEDGEMENT

Authors acknowledge the department of Cell Biology and Molecular Genetics for providing all the essentials for the successful completion of this work.

## CONFLICTS OF INTEREST/COMPETING INTERESTS

Authors declare no conflict of interest

## ETHICS CLEARANCE

No: SDUAHER/KRL/Res. Project/128/ 2017-'18

## REFERENCES

1. Jeevanandam J, Barhoum A, Chan YS, Dufresne A, Danquah MK. Review on nanoparticles and nanostructured materials: history, sources, toxicity and regulations. *Beilstein J Nanotechnol.* 2018;9:1050-74.
2. Heydary V, Navaei-Nigjeh M, Rahimifard M, Mohammadirad A, Baeri M, Abdollahi M. Biochemical and molecular evidences on the protection by magnesium oxide nanoparticles of chlorpyrifos-induced apoptosis in human lymphocytes. *J Res Med Sci.* 2015;20(11):1021-31.

3. Kuppusamy P, Yusoff MM, Maniam GP, Govindan N. Biosynthesis of metallic nanoparticles using plant derivatives and their new avenues in pharmacological applications - An updated report. *Saudi Pharm J*. 2016;24(4):473-84.
4. Cai L, Chen J, Liu Z, Wang H, Yang H, Ding W. Magnesium Oxide Nanoparticles: Effective Agricultural Antibacterial Agent Against *Ralstonia solanacearum*. *Front Microbiol*. 2018;9:790-.
5. P K, N P, H S N, A V M K. Comparative analysis of transition and post transition metal mediated *Allamanda cathartica* L latex nanoparticles on human peripheral blood mononuclear cells. *Advances in Natural Sciences: Nanoscience and Nanotechnology*. 2020;11(1):015016.
6. Chandreyi Ghosh, Labani Hazra, Sudip Kumar Nag, Sayantan Sil, Alolika Dutta, Swagata Biswas, Pranabesh Ghosh & Sirshendu Chatterjee. *Allamanda cathartica* Linn. Apocynaceae: A mini review. *International Journal of Herbal Medicine*, 2019; 7(4), 29-33.
7. Barbagallo M, Dominguez LJ. Magnesium and type 2 diabetes. *World J Diabetes*. 2015;6(10):1152-7.
8. Patil SP. *Calotropis gigantea* assisted green synthesis of nanomaterials and their applications: a review. *Beni-Suef University Journal of Basic and Applied Sciences*. 2020;9(1).
9. Harborne JB. *Phytochemical Methods: A Guide to Modern Techniques of Plant Analysis*, 2<sup>nd</sup> edn, UK: Chapman and Hall, London, 1973; pp. 1-288. <https://doi.org/10.1007/978-94-009-5570-7>
10. Banerjee P, Satapathy M, Mukhopahayay A, Das P. Leaf extract mediated green synthesis of silver nanoparticles from widely available Indian plants: synthesis, characterization, antimicrobial property and toxicity analysis. *Bioresources and Bioprocessing*. 2014;1(1).
11. de F Navarro Schmidt D, Yunes R.A, Schaab EH, Malheiros A, Cechinel Filho V, Franchi GC Jr, Nowill AE, Cardoso AA, Yunes J. Evaluation of the antiproliferative effect the extracts of *Allamanda blanchetti* and *A. schottii* on the growth of leukemic and endothelial cells. *Journal of Pharmacy and Pharmaceutical Sciences*, 2006; 9(2), 200-208. <https://www.ncbi.nlm.nih.gov/pubmed/16959189>
12. Strober W. Trypan Blue Exclusion Test of Cell Viability. *Current Protocols in Immunology*: John Wiley & Sons, Inc.; 2001.
13. Pattern R, Hirzel A. Apoptosis DNA fragmentation analysis protocol Abcam, Apoptosis DNA fragmentation analysis protocol – 1. 2017. (<http://docs.abcam.com/pdf/protocols/apoptosis-dna-fragmentation-analysis-protocol.pdf>)
14. Kelly KL, Coronado E, Zhao LL, Schatz GC. The Optical Properties of Metal Nanoparticles: The Influence of Size, Shape, and Dielectric Environment. *The Journal of Physical Chemistry B*. 2002;107(3):668-77.
15. Philip D. Synthesis and spectroscopic characterization of gold nanoparticles. *Spectrochimica Acta Part A: Molecular and Biomolecular Spectroscopy*. 2008;71(1):80-5.
16. Vanden Bout DA. *Metal Nanoparticles: Synthesis, Characterization, and Applications* Edited by Daniel L. Feldheim (North Carolina State University) and Colby A. Foss, Jr. (Georgetown University). Marcel Dekker, Inc.: New York and Basel. 2002. x+ 338 pp. \$150.00. ISBN: 0-8247-0604-8. *Journal of the American Chemical Society*. 2002;124(26):7874-5.
17. Dobrucka R. Synthesis of MgO Nanoparticles Using *Artemisia abrotanum* Herba Extract and Their Antioxidant and Photocatalytic Properties. *Iranian Journal of Science and Technology, Transactions A: Science*. 2016;42(2):547-55.
18. Halbus AF, Horozov TS, Paunov VN. Controlling the Antimicrobial Action of Surface Modified Magnesium Hydroxide Nanoparticles. *Biomimetics (Basel)*. 2019;4(2):41.
19. Vinardell MP, Mitjans M. Antitumor Activities of Metal Oxide Nanoparticles. *Nanomaterials (Basel)*. 2015;5(2):1004-21.
20. Behzadi E, Sarsharzadeh R, Nouri M, Attar F, Akhtari K, Shahpasand K, et al. Albumin binding and anticancer effect of magnesium oxide nanoparticles. *Int J Nanomedicine*. 2018;14:257-70.
21. Safaei M, Taran M, Rezaei R, Mansouri K, Mozaffari HR, Imani MM, et al. Synthesis and anticancer properties of bacterial cellulose-magnesium oxide bionanocomposite. *Current Issues in Pharmacy and Medical Sciences*. 2019;32(1):29-33.
22. Stoimenov PK, Klinger RL, Marchin GL, Klabunde KJ. Metal Oxide Nanoparticles as Bactericidal Agents. *Langmuir*. 2002;18(17):6679-86.
23. Ge S, Dong Q, Shen Y, Wang H, Yin T, Wang G, et al. Cytotoxic effects of MgO nanoparticles on human umbilical vein endothelial cells in vitro. *IET Nanobiotechnology*. 2011;5(2):36-40.
24. Krishnamoorthy K, Moon JY, Hyun HB, Cho SK, Kim S-J. Mechanistic investigation on the toxicity of MgO nanoparticles toward cancer cells. *Journal of Materials Chemistry*. 2012;22(47):24610.
25. Sun J, Wang S, Zhao D, Hun FH, Weng L, Liu H. Cytotoxicity, permeability, and inflammation of metal oxide nanoparticles in human cardiac microvascular endothelial cells. *Cell Biology and Toxicology*. 2011;27(5):333-42.
26. Lai JCK, Lai MB, Jandhyam S, Dukhande VV, Bhushan A, Daniels CK, Leung SW. Exposure to titanium dioxide and other metallic oxide nanoparticles induces cytotoxicity on human neural cells and fibroblasts. *International Journal of Nanomedicine*, 2008; 3(4), 533-545. doi:10.2147/ijn.s3234. PMID: 19337421. PMID: PMC2636591
27. Martinez-Boubeta C, Balcells L, Cristòfol R, Sanfeliu C, Rodríguez E, Weissleder R, et al. Self-assembled multifunctional Fe/MgO nanospheres for magnetic resonance imaging and hyperthermia. *Nanomedicine: Nanotechnology, Biology and Medicine*. 2010;6(2):362-70.
28. Chalkidou A, Simeonidis K, Angelakeris M, Samaras T, Martinez-Boubeta C, Balcells L, et al. In vitro

- application of Fe/MgO nanoparticles as magnetically mediated hyperthermia agents for cancer treatment. *Journal of Magnetism and Magnetic Materials*. 2011;323(6):775-80.
29. Lei ZQ, Li L, Li GJ, Leung CW, Shi J, Wong CM, et al. Liver cancer immunoassay with magnetic nanoparticles and MgO-based magnetic tunnel junction sensors. *Journal of Applied Physics*. 2012;111(7):07E505.
  30. Di D-R, He Z-Z, Sun Z-Q, Liu J. A new nano-cryosurgical modality for tumor treatment using biodegradable MgO nanoparticles. *Nanomedicine: Nanotechnology, Biology and Medicine*. 2012;8(8):1233-41.
  31. Hasbullah NI, Mazatulikhma MZ, Kamarulzaman N. Nanotoxicity of Magnesium Oxide on Human Neuroblastoma SH-SY5Y Cell Lines. *Advanced Materials Research*. 2013;667:160-4.
  32. Lesniak A, Fenaroli F, Monopoli MP, Åberg C, Dawson KA, Salvati A. Effects of the Presence or Absence of a Protein Corona on Silica Nanoparticle Uptake and Impact on Cells. *ACS Nano*. 2012;6(7):5845-57.